

## Fluorescent Probes

International Edition: DOI: 10.1002/anie.201703298  
German Edition: DOI: 10.1002/ange.201703298

## Synthesis of a Fluorescent Analogue of Paclitaxel that Selectively Binds Microtubules and Sensitively Detects Efflux by P-Glycoprotein

Molly M. Lee<sup>+</sup>, Zhe Gao<sup>+</sup>, and Blake R. Peterson\*Dedicated to Professor François Diederich on the occasion of his 65<sup>th</sup> birthday

**Abstract:** The anticancer drug paclitaxel (Taxol) exhibits paradoxical and poorly understood effects against slow-growing tumors. To investigate its biological activity, fluorophores such as Oregon Green have been linked to this drug. However, this modification increases its polarity by approximately 1000-fold and reduces the toxicity of Taxol towards cancer cell lines by over 200-fold. To construct more drug-like fluorescent probes suitable for imaging by confocal microscopy and analysis by flow cytometry, we synthesized derivatives of Taxol linked to the drug-like fluorophore Pacific Blue (PB). We found that PB-Gly-Taxol bound the target protein  $\beta$ -tubulin with both high affinity *in vitro* and high specificity in living cells, exhibited substantial cytotoxicity towards HeLa cells, and was a highly sensitive substrate of the multidrug resistance transporter P-glycoprotein (P-gp).

**P**aclitaxel (Taxol, Figure 1), a natural product first isolated from the bark of the yew tree *Taxus brevifolia*, is one of the most effective treatments for ovarian, breast, and lung cancers.<sup>[1]</sup> By binding the protein  $\beta$ -tubulin, this drug stabilizes microtubules in the cytosol, inhibits microtubule polymerization dynamics, and triggers cellular death through apoptosis.<sup>[1]</sup> Although Taxol is widely used as a therapeutic, the mechanisms underlying its selective cytotoxicity towards cancer cells remain incompletely understood. Taxol and related compounds exhibit antimetabolic activity against rapidly dividing cancer cell lines and xenografts that double every 1–12 days,<sup>[2]</sup> thus suggesting that effects against rapidly proliferating cells might provide selectivity for tumors in human patients. However, these drugs also show major effects against slow-growing tumors (median doubling time of ca. 147 days) in patients,<sup>[2]</sup> while sparing rapidly proliferating normal cells in the bone marrow, gut, and other tissues. This surprising selectivity has been termed the “proliferation-rate paradox”.<sup>[3]</sup>

To probe the anticancer effects of Taxol, fluorescent analogues<sup>[4–15]</sup> have been reported. The most extensively studied derivative, a commercially available compound termed Flutax-2 (Figure 1), comprises Taxol linked at the 7-

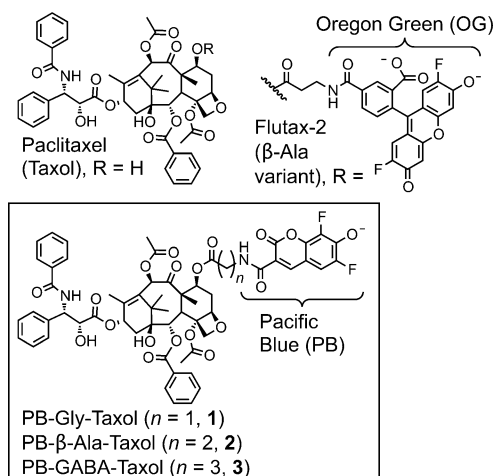


**Figure 1.** Structures of paclitaxel (Taxol), the commercially available green fluorescent taxoid Flutax-2, and Pacific Blue derivatives (1–3).

position through a  $\beta$ -Ala ester to the fluorophore Oregon Green (OG). This  $\beta$ -Ala linker was first used by Nicolaou and co-workers<sup>[8]</sup> to prepare some of the earliest fluorescent taxoids. Esters derived from L-Ala<sup>[14]</sup> and other substituents<sup>[5,10]</sup> have also been used to link fluorophores to Taxol at the 7-position. The term Flutax-2 has also been used to describe a related probe where Taxol is linked to OG via an L-Ala ester [here termed Flutax-2 (L-Ala)].<sup>[7]</sup> The side chain of Taxol has also been linked to the BODIPY fluorophore,<sup>[16,17]</sup> but these probes are generally not considered suitable for imaging in living cells.

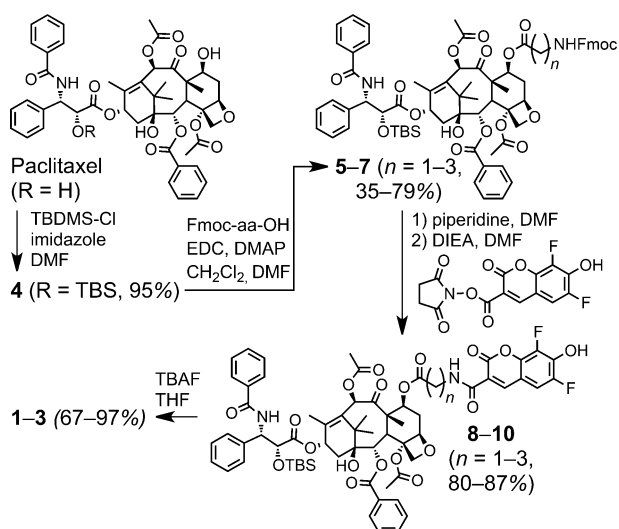
At physiological pH, OG exists as a highly polar dianion (Figure 1).<sup>[18]</sup> In Flutax-2, this increases the polarity of Taxol by almost 1000-fold, altering its calculated octanol–water distribution/partition coefficient from  $c\text{Log}D_{\text{pH}7.4} = 2.9$  (Taxol) to  $c\text{Log}D_{\text{pH}7.4} = 0.0$  (Flutax-2). Given that most small-molecule drugs are moderately hydrophobic ( $c\text{Log}D_{\text{pH}7.4} \approx 2$ ), which facilitates passive diffusion across membranes, Flutax-2 is not very drug-like. To provide more drug-like probes, we report here studies of Taxol linked to the fluorophore Pacific Blue (PB, Figure 1),<sup>[19]</sup> which is substantially smaller and less polar than OG ( $c\text{Log}D_{\text{pH}7.4} = 2.0$  for PB-Gly-Taxol (1); Figure 1).

To examine whether modification of Taxol with PB might more effectively recapitulate its biological activities, we synthesized probes 1–3 (Figure 1) via the known<sup>[20]</sup> TBS-protected derivative 4 (Scheme 1). PB was chosen because, unlike most other coumarins, its photophysical and chemical

[\*] Dr. M. M. Lee,<sup>[+]</sup> Z. Gao,<sup>[+]</sup> Prof. Dr. B. R. Peterson  
Department of Medicinal Chemistry, The University of Kansas  
Lawrence, KS 66045 (USA)  
E-mail: brpeters@ku.edu

[+] These authors contributed equally to this work.

Supporting information and the ORCID identification number(s) for the author(s) of this article can be found under:  
<https://doi.org/10.1002/anie.201703298>.



**Scheme 1.** Synthesis of PB-Taxols 1–3.

properties ( $\lambda_{\text{Ex}} = 400 \text{ nm}$ ,  $\lambda_{\text{Em}} = 447 \text{ nm}$ ,  $\epsilon = 29500 \text{ M}^{-1} \text{ cm}^{-1}$ ,  $\text{QY} = 0.75$ , phenol  $\text{p}K_{\text{a}} = 3.7$ )<sup>[19]</sup> allow it to be efficiently excited at 405 nm with violet lasers found on many confocal microscopes and flow cytometers. Additionally, PB can be readily synthesized in gram quantities.<sup>[21]</sup> Because taxoids modified at the 7-position can retain high affinity for microtubules,<sup>[22]</sup> PB was linked at this position via amino acids that differ subtly in the number of methylenes between the amine and the carbonyl. Optical spectroscopy confirmed that the fluorescence properties of 1–3 are similar to PB, whereas Flutax-2 is similar to OG (Figure S1 in the Supporting Information).

Flutax-2 (L-Ala) has been reported to bind human  $\beta$ -tubulin with an apparent  $K_{\text{d}} = 14 \text{ nM}$ , as quantified by changes in fluorescence anisotropy.<sup>[23]</sup> BODIPY-modified paclitaxel is known to exhibit enhanced fluorescence upon binding to this protein,<sup>[24]</sup> and we measured the affinities of 1–3 for cross-linked microtubules<sup>[7]</sup> from bovine brain using a fluorescence-enhancement method (Figure 2). Curve fitting of the equilibrium binding curves yielded apparent  $K_{\text{d}}$  values of  $34 \pm 6 \text{ nM}$  for PB-Gly-Taxol (1),  $63 \pm 8 \text{ nM}$  for PB- $\beta$ -Ala-Taxol (2), and  $265 \pm 54 \text{ nM}$  for PB-GABA-Taxol (3) in GAB<sup>[7]</sup> buffer.

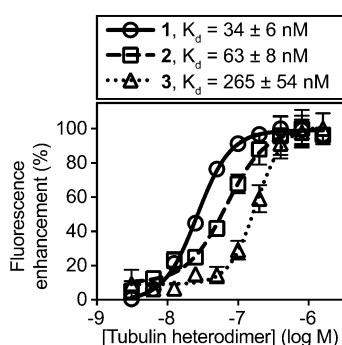


**Figure 2.** Quantification of the affinities ( $K_{\text{d}}$ ) of 1–3 (25 nM) for cross-linked microtubules by enhancement of fluorescence. Binding studies were conducted in aqueous GAB buffer (pH 6.5). PB was excited at 405 nm and emission was measured at and above 450 nm.

and  $265 \pm 54 \text{ nM}$  for PB-GABA-Taxol (3) in GAB<sup>[7]</sup> buffer. Addition of excess paclitaxel ( $10 \mu\text{M}$ ) blocked this fluorescence enhancement, thus demonstrating that 1–3 bind  $\beta$ -tubulin at the same site as paclitaxel (data not shown).

To attempt to rationalize differences in the affinities of 1–3, these compounds were docked, using Autodock vina,<sup>[25]</sup> to the Taxol-binding site from a recent cryo-EM structure<sup>[26]</sup> of  $\beta$ -tubulin bound to Taxol. These modeling studies suggested that linked fluorophores may favorably insert into a pocket near the Taxol-binding site (Figure 3). Although docking did

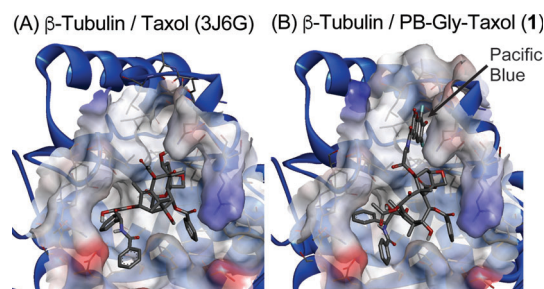


**Figure 3.** Comparison of a published structure (PDB ID: 3J6G) of Taxol bound to  $\beta$ -tubulin (A) with a model (B) of  $\beta$ -tubulin docked to 1. In (B), a docking pose of 1 is shown where the side-chain orientations are similar to those of Taxol in panel (A), and the PB moiety of 1 engages a neighboring pocket on the protein surface.

not readily correlate the higher affinity of 1 compared to 2 and 3 with greater or lesser engagement of this pocket by the fluorophore, the affinities determined experimentally suggest that conformational restriction of the longer and more flexible linkers of 2 and 3 might reduce the affinity upon binding of PB to the same pocket.

The cytotoxicity of fluorescent taxoids towards HeLa cervical carcinoma cells (Figure 4) and multidrug-resistant HCT-15 colorectal adenocarcinoma cells (Figure S3) was evaluated. These cell lines were treated for 48 h, cellular

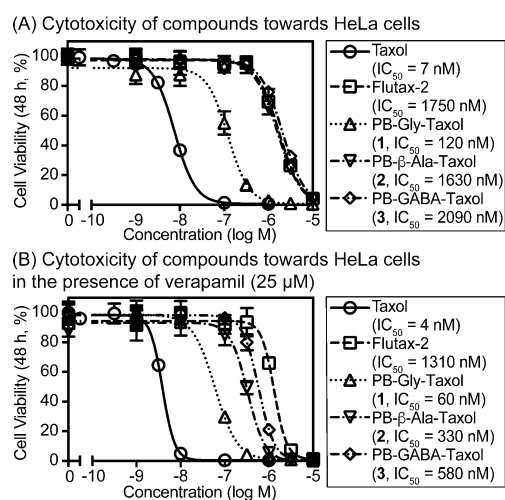


**Figure 4.** Analysis of cytotoxicity. HeLa cells were treated with compounds in the absence (A) or presence (B) of verapamil ( $25 \mu\text{M}$ ) for 48 h and cellular viability measured by flow cytometry.

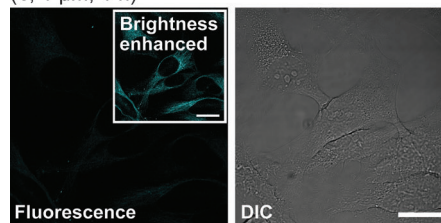
viability was analyzed by flow cytometry, and Taxol was used as a positive control. HCT-15 cells overexpress P-glycoprotein (P-gp, MDR1, ABCB1), and because Taxol is a substrate of this efflux transporter,<sup>[27]</sup> we further measured cytotoxicity in the presence of the P-gp inhibitor verapamil<sup>[28]</sup> (Figure 4, panel B, and Figure S3). Among the fluorescent probes, **1** was uniquely toxic, with  $IC_{50} = 120$  nM in the absence of and  $IC_{50} = 60$  nM in the presence of verapamil (25  $\mu$ M) in HeLa cells. In HCT-15 cells, verapamil (25  $\mu$ M) enhanced the toxicity of **1** by 41-fold (from  $IC_{50} = 3.7$   $\mu$ M to  $IC_{50} = 90$  nM). Control experiments confirmed that verapamil itself ( $IC_{50} > 75$   $\mu$ M at 48 h, Figure S3) did not contribute to these cytotoxic effects. HeLa cells express low levels of P-gp<sup>[29]</sup> compared to HCT-15 cells, and this enhanced cytotoxicity mediated by verapamil suggested that **1–3** might be highly efficient substrates of this drug efflux transporter. Flutax-2 is known to be a substrate of P-gp,<sup>[30]</sup> but in HeLa cells treated with verapamil, Flutax-2 was the least cytotoxic ( $IC_{50} = 1310$  nM), likely due to its higher polarity and associated lower cellular permeability. Flutax-2 (L-Ala) has been previously reported to exhibit cytotoxic  $IC_{50}$  values of 800 nM against drug-sensitive A2780 cells and more than 20  $\mu$ M against drug-resistant A2780AD cells.<sup>[9]</sup> Because **1** appeared to most closely mimic Taxol, it became the focus of further studies.

To examine the subcellular distribution of **1**, we imaged HeLa cells by confocal laser scanning microscopy (Figure 5). After treating cells with **1** (1  $\mu$ M, 1 h), co-treatment with verapamil dramatically enhanced cellular fluorescence in a dose-dependent manner (Figures 5 and S2), revealing intricate networks of microtubules in living cells. The distinct spectral profiles of PB and OG were used to further examine the colocalization of **1** and Flutax-2 (Figures 5 C). Whereas **1** bound microtubules with very high specificity, Flutax-2 additionally conferred punctate fluorescence that did not colocalize with **1**. This lower specificity of Flutax-2 is consistent with a prior report<sup>[10]</sup> of its off-target accumulation in the Golgi apparatus.

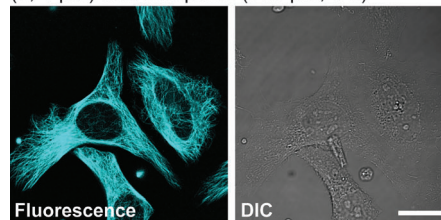
Overexpression of P-gp frequently confers resistance to the antiproliferative effects of Taxol.<sup>[31]</sup> To further investigate whether **1** is a substrate of P-gp, we transiently transfected PC-3 cells, which lack this transporter,<sup>[32]</sup> with a plasmid (pHaMDR-EGFP) encoding P-gp fused to enhanced green fluorescent protein (EGFP). Unlike HeLa cells, imaging of PC-3 cells treated with **1** (1  $\mu$ M) revealed strong blue fluorescence in the absence of verapamil (Figure S4). However, in cells expressing green fluorescent P-gp-EGFP, a decrease in blue fluorescence was observed that was dependent on the level of P-gp-EGFP expression (Figure S4), thus indicating that **1** is a potent substrate of this transporter. Treatment with verapamil reversed this effect by blocking P-gp to prevent the efflux of **1**.

We additionally investigated the efflux of **1** in HCT-15 cells that express high levels of P-gp.<sup>[29]</sup> Compound **1** was compared with rhodamine 123 (Rho123), a common P-gp substrate that accumulates in mitochondria.<sup>[33]</sup> As shown in Figure 6, the cells were analyzed after treatment with **1** (1  $\mu$ M), Rho123 (1  $\mu$ M), and verapamil (0, 25, 100  $\mu$ M) by confocal microscopy and flow cytometry. Whereas the fluorescence of Rho123 increased by only 3-fold in the

(A) Treatment of HeLa cells with PB-Gly-Taxol (**1**, 1  $\mu$ M, 1 h)



(B) Treatment of HeLa cells with PB-Gly-Taxol (**1**, 1  $\mu$ M) and verapamil (100  $\mu$ M, 1 h)



(C) Treatment of HeLa cells with PB-Gly-Taxol (**1**, 1  $\mu$ M), Flutax-2 (5  $\mu$ M) and verapamil (25  $\mu$ M, 1 h)

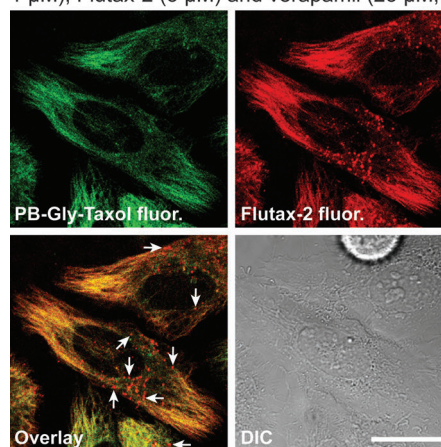


**Figure 5.** A–C) Confocal laser scanning and differential interference contrast (DIC) microscopy of HeLa cells treated with **1** (1  $\mu$ M, 1 h). A,B) Images of cells in the absence (A) and in the presence (B) of verapamil (100  $\mu$ M). In the inset of (A), the brightness was enhanced to reveal the weak fluorescence of **1** resulting from efflux. C) Cells were further treated with verapamil (25  $\mu$ M) and Flutax-2 (5  $\mu$ M) to examine colocalization. Arrows indicate punctate fluorescence of Flutax-2. Scale bar: 25  $\mu$ m.

presence of verapamil (at 25 or 100  $\mu$ M), the fluorescence of **1** increased by 7-fold at 25  $\mu$ M and 15-fold at 100  $\mu$ M verapamil. Moreover, in HeLa cells, **1** could detect low levels of P-gp activity that were undetectable by Rho123 (Figures 6D and Figure S5), enhancing the fluorescence by 10-fold at 25  $\mu$ M verapamil and 23-fold at 100  $\mu$ M verapamil, thus indicating that **1** is a uniquely sensitive sensor of this efflux transporter.

In contrast to Flutax-2, which is only weakly cytotoxic and exhibits low cellular permeability due to the high polarity of the appended OG fluorophore, the more drug-like PB-Gly-Taxol (**1**) substantially recapitulates the cytotoxic, tubulin-binding and P-gp-mediated efflux activity of the parent anticancer drug. Because PB can be efficiently detected and analyzed by confocal microscopy and flow cytometry, this

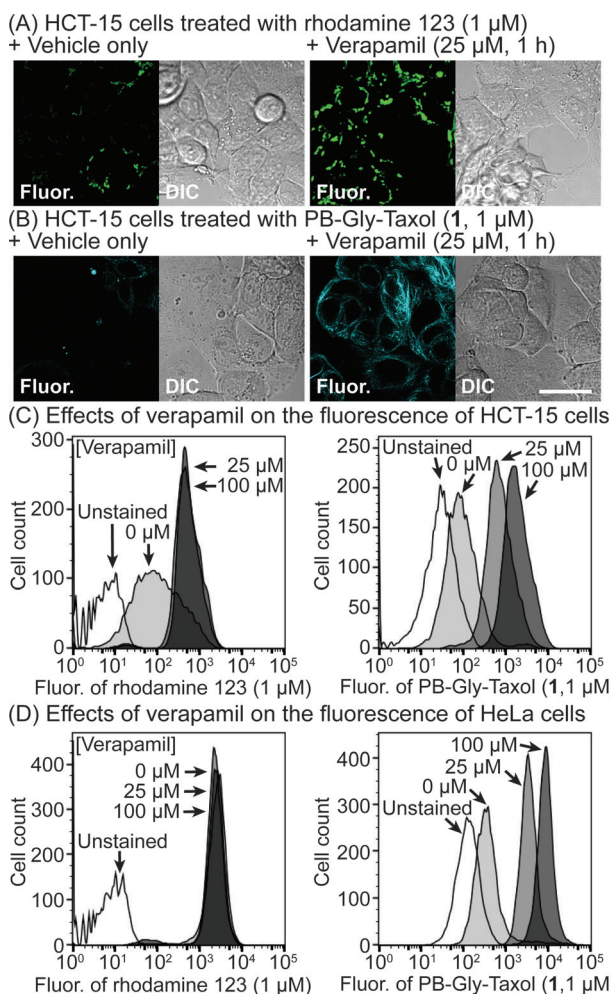


**Figure 6.** A,B) Confocal laser scanning and DIC microscopy of HCT-15 cells treated with the P-gp substrates rhodamine 123 (A) and 1 (B). C,D) Analysis of HCT-15 (C) and HeLa (D) cells treated with rhodamine 123 (left panels) or 1 (right panels) by flow cytometry. Concentrations of added verapamil are shown. Scale bar: 25  $\mu\text{m}$ .

probe offers a new tool for studies of the paradoxical anticancer effects of Taxol.

### Acknowledgements

We thank Prof. Dr. Liang Xu for the HCT-15 cells, Prof. Dr. Matthew Levy for the PC-3 cells, and Dr. Michael Gottesman for the pHaMDR-EGFP plasmid. B. Peterson acknowledges support from the NIH (P20-GM103638, P20-GM103418, and R01-CA211720), and the G. Harold and Leila Y. Mathers Charitable Foundation. MML acknowledges support from the NIH Dynamic Aspects of Chemical Biology Training Grant at the University of Kansas (T32-GM08545).

### Conflict of interest

The authors declare no conflict of interest.

**Keywords:** antitumor agents · confocal microscopy · drug design · fluorescent probes · paclitaxel

- [1] C. C. Rohena, S. L. Mooberry, *Nat. Prod. Rep.* **2014**, *31*, 335–355.
- [2] E. Komlodi-Pasztor, D. Sackett, J. Wilkerson, T. Fojo, *Nat. Rev. Clin. Oncol.* **2011**, *8*, 244–250.
- [3] T. J. Mitchison, *Mol. Biol. Cell* **2012**, *23*, 1–6.
- [4] I. Barasoain, J. F. Diaz, J. M. Andreu, *Methods Cell Biol.* **2010**, *95*, 353–372.
- [5] J. F. Díaz, I. Barasoain, A. A. Souto, F. Amat-Guerri, J. M. Andreu, *J. Biol. Chem.* **2005**, *280*, 3928–3937.
- [6] I. Barasoain, A. M. García-Carril, R. Matesanz, G. Maccari, C. Trigili, M. Mori, J.-Z. Shi, W.-S. Fang, J. M. Andreu, M. Botta, J. F. Díaz, *Chem. Biol.* **2010**, *17*, 243–253.
- [7] J. F. Diaz, R. Strobe, Y. Engelborghs, A. A. Souto, J. M. Andreu, *J. Biol. Chem.* **2000**, *275*, 26265–26276.
- [8] R. K. Guy, Z. A. Scott, R. D. Sloboda, K. C. Nicolaou, *Chem. Biol.* **1996**, *3*, 1021–1031.
- [9] X. Li, I. Barasoain, R. Matesanz, J. F. Diaz, W. S. Fang, *Bioorg. Med. Chem. Lett.* **2009**, *19*, 751–754.
- [10] S. Duchi, P. Dambrosio, E. Martella, G. Sotgiu, A. Guerrini, E. Lucarelli, A. Pessina, V. Cocce, A. Bonomi, G. Varchi, *Bioconjugate Chem.* **2014**, *25*, 649–655.
- [11] G. Lukinavičius, L. Reymond, E. D'Este, A. Masharina, F. Gottfert, H. Ta, A. Güther, M. Fournier, S. Rizzo, H. Waldmann, C. Blaukopf, C. Sommer, D. W. Gerlich, H.-D. Arndt, S. W. Hell, K. Johnsson, *Nat. Methods* **2014**, *11*, 731–733.
- [12] S. Sengupta, T. C. Boge, G. I. Georg, R. H. Himes, *Biochemistry* **1995**, *34*, 11889–11894.
- [13] Y. Han, A. G. Chaudhary, M. D. Chordia, D. L. Sackett, B. Perez-Ramirez, D. G. Kingston, S. Bane, *Biochemistry* **1996**, *35*, 14173–14183.
- [14] A. A. Souto, A. U. Acuna, J. M. Andreu, I. Barasoain, M. Abal, F. AmatGuerrri, *Angew. Chem. Int. Ed. Engl.* **1995**, *34*, 2710–2712; *Angew. Chem.* **1995**, *107*, 2910–2912.
- [15] E. Baloglu, D. G. Kingston, P. Patel, S. K. Chatterjee, S. L. Bane, *Bioorg. Med. Chem. Lett.* **2001**, *11*, 2249–2252.
- [16] C. Martin, J. Walker, A. Rothnie, R. Callaghan, *Br. J. Cancer* **2003**, *89*, 1581–1589.
- [17] B. Gao, A. Russell, J. Beesley, X. Q. Chen, S. Healey, M. Henderson, M. Wong, C. Emmanuel, L. Galletta, S. E. Johnatty, D. Bowtell, M. Haber, M. Norris, P. Harnett, G. Chenevix-Trench, R. L. Balleine, A. deFazio, *Sci. Rep.* **2014**, *4*, 4669.
- [18] W. C. Sun, K. R. Gee, D. H. Klaubert, R. P. Haugland, *J. Org. Chem.* **1997**, *62*, 6469–6475.
- [19] W.-C. Sun, K. R. Gee, R. P. Haugland, *Bioorg. Med. Chem. Lett.* **1998**, *8*, 3107–3110.
- [20] N. F. Magri, D. G. I. Kingston, *J. Nat. Prod.* **1988**, *51*, 298–306.
- [21] M. M. Lee, B. R. Peterson, *ACS Omega* **2016**, *1*, 1266–1276.
- [22] X. Xiao, J. Wu, C. Trigili, H. Chen, J. W. K. Chu, Y. Zhao, P. Lu, L. Sheng, Y. Li, F. J. Sharom, I. Barasoain, J. F. Diaz, W.-s. Fang, *Bioorg. Med. Chem. Lett.* **2011**, *21*, 4852–4856.
- [23] R. M. Buey, E. Calvo, I. Barasoain, O. Pineda, M. C. Edler, R. Matesanz, G. Cerezo, C. D. Vanderwal, B. W. Day, E. J. Sorensen, J. A. Lopez, J. M. Andreu, E. Hamel, J. F. Diaz, *Nat. Chem. Biol.* **2007**, *3*, 117–125.
- [24] R. Rouzier, R. Rajan, P. Wagner, K. R. Hess, D. L. Gold, J. Stec, M. Ayers, J. S. Ross, P. Zhang, T. A. Buchholz, H. Kuerer, M. Green, B. Arun, G. N. Hortobagyi, W. F. Symmans, L. Pusztai, *Proc. Natl. Acad. Sci. USA* **2005**, *102*, 8315–8320.
- [25] O. Trott, A. J. Olson, *J. Comput. Chem.* **2010**, *31*, 455–461.
- [26] G. M. Alushin, G. C. Lander, E. H. Kellogg, R. Zhang, D. Baker, E. Nogales, *Cell* **2014**, *157*, 1117–1129.

- [27] S. H. Jang, M. G. Wientjes, J. L.-S. Au, *J. Pharmacol. Exp. Ther.* **2001**, 298, 1236–1242.
- [28] T. Tsuruo, H. Iida, S. Tsukagoshi, Y. Sakurai, *Cancer Res.* **1981**, 41, 1967–1972.
- [29] I. V. Lebedeva, P. Pande, W. F. Patton, *PLoS ONE* **2011**, 6, e22429.
- [30] G. Patwardhan, V. Gupta, J. Huang, X. Gu, Y. Y. Liu, *Biochem. Pharmacol.* **2010**, 80, 72–79.
- [31] P. D. W. Eckford, F. J. Sharom, *Chem. Rev.* **2009**, 109, 2989–3011.
- [32] J. P. van Brussel, G. J. van Steenbrugge, J. C. Romijn, F. H. Schröder, G. H. J. Mickisch, *Eur. J. Cancer* **1999**, 35, 664–671.
- [33] S. Forster, A. E. Thumser, S. R. Hood, N. Plant, *PLoS ONE* **2012**, 7, e33253.

Manuscript received: March 29, 2017

Final Article published: ■ ■ ■ ■, ■ ■ ■ ■ ■ ■

## Communications

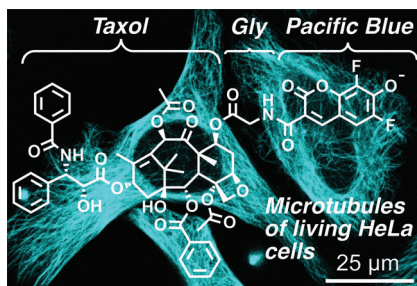


## Fluorescent Probes

M. M. Lee, Z. Gao,

B. R. Peterson\*     

Synthesis of a Fluorescent Analogue of Paclitaxel that Selectively Binds Microtubules and Sensitive Detects Efflux by P-Glycoprotein



The fluorophore normally linked to the anticancer drug paclitaxel (Taxol) to investigate its biological activity significantly alters its properties. To construct more drug-like fluorescent probes suitable for confocal microscopy and flow cytometry, Taxol was linked to the drug-like fluorophore Pacific Blue (PB). PB-Gly-Taxol bound the target protein  $\beta$ -tubulin with high affinity and high specificity, and exhibited substantial cytotoxicity towards HeLa cells.